

Chapter 4 Global Phase Diagrams

Global phase diagrams provide a systematic tool to investigate the phase behaviour of simple as well as complex mixtures. In the early years the method was applied to simple binary fluids mixtures (van Konynenburg and Scott, 1980; Deiters and Pegg, 1989; Kraska and Deiters, 1991; Yelash and Kraska, 1998; Kolafa et al., 1998; Lamm and Hall, 2001) , whereas recent development focuses on complex systems such as polar substances, ionic systems, polymer solutions or blends (Kraska, 1996; Yelash and Kraska, 1999; Kolafa et al., 1999; Imre et al., 1999; Polishuk et al., 2000, 2002).

To generate a global phase diagram reduced differences of the molecular parameters of the mixture are plotted against each other. The boundaries between the different types of phase behaviour can be obtained by calculating high order thermodynamic states which represent transition states between different types of phase behaviour. As a result one obtains a map which provides an overview of the phase behaviour within the validity of a molecular model. Full continuity of the molecular parameters is possible only in theoretical work. In the experimental approach only a series of discrete systems can be investigated. This limitation can be overcome by using in multi-component mixtures binaries as pseudo pure substances which allow the effective variation of a molecular property with mole fraction of the pseudo-pure substances.

There are two main areas in which progress has been made in recent years. The topological investigation of the complete global phase diagram is necessary for its basic understanding and the investigation of the properties of a certain molecular

model. Another direction is the application of the method for the understanding of selected phenomena in the science of phase equilibria, which are located in a limited region in the global phase diagram.

4.1 Classification of Description of Phase Behaviour of Binary Mixtures

As discussed in the Chapter 2 (Figure 2.3), nine general types of phase behaviour were found. Seven types (types *I* → *VI*, and *VIII*) of binary mixtures are encountered experimentally, whereas the other two types (*Vm* and *VII*) were reported from equations of state calculations (Kraska and Deiters, 1991; Yelash and Kraska, 1998; Wang et al., 2000; Lamm and Hall, 2001). There are various sub-classes of the main type of phase behaviour, depending on the positions of the main critical locus (Rowlinson and Swinton, 1982). We will discuss these sub-classes here.

4.1.1 Type I Phase Behaviour

The simplest possible behaviour is type I phase behaviour which is shown in Figure 4.1 (Rowlinson and Swinton, 1982). Typical examples are mainly mixtures of non-dipolar molecules such as carbon dioxide + oxygen (Muirbrook and Prausnitz, 1965), methane + ethane (Wichterle and Kobayashi, 1972), methane + nitrogen (Stryjek et al., 1974) and argon + krypton (Schouten et al., 1975), and a few examples of type I behaviour are known containing polar substances such as sulphur dioxide + chloromethane and hydrogen chloride + dimethylether (Prausnitz et al., 1999).

Type I mixtures can be conveniently subdivided into five types by considering the shape of the critical curve, and into two types by azeotropy (azeotropy is shown in 4.2.1). Figure 4.1 represents these possible type I critical phase behaviours in p-T projection.

Mixture of curve (a) (type I_a) is convex upwards and frequently exhibits a maximum in the (p, T) projection extremely common among type I systems and occur whenever there are moderately large differences between the critical temperatures or volumes of the pure components. Examples of type I_a mixtures are obtained by combining n-hexane with n-heptane, n-octane, n-decane, n-tridecane or n-tetradecane (Rowlinson and Swinton, 1982). Furthermore, mixtures of simple molecules also frequently correspond to curve (a) behaviour of type I, such as argon + methane, argon + krypton and krypton + methane (Schouten et al., 1975).

Mixtures approximating to curve (β) (type I_β), where the critical locus is almost linear in the (p, T) projection, are usually formed from substances with very similar critical properties. Typical examples of type I_β are carbon dioxide + nitrous oxide and benzene + toluene (Rowlinson and Swinton, 1982).

The critical curve of type I_γ (curve γ in Figure 4.1) concaves upwards and may exhibit minimum in the p-T projection. Such behaviour is found for binary mixtures of a polar with a non-polar substance, and for some mixtures of aromatic hydrocarbons with aliphatic or alicyclic hydrocarbons such as propane + hydrogen sulphide and methanol + benzene (Rowlinson and Swinton, 1982).

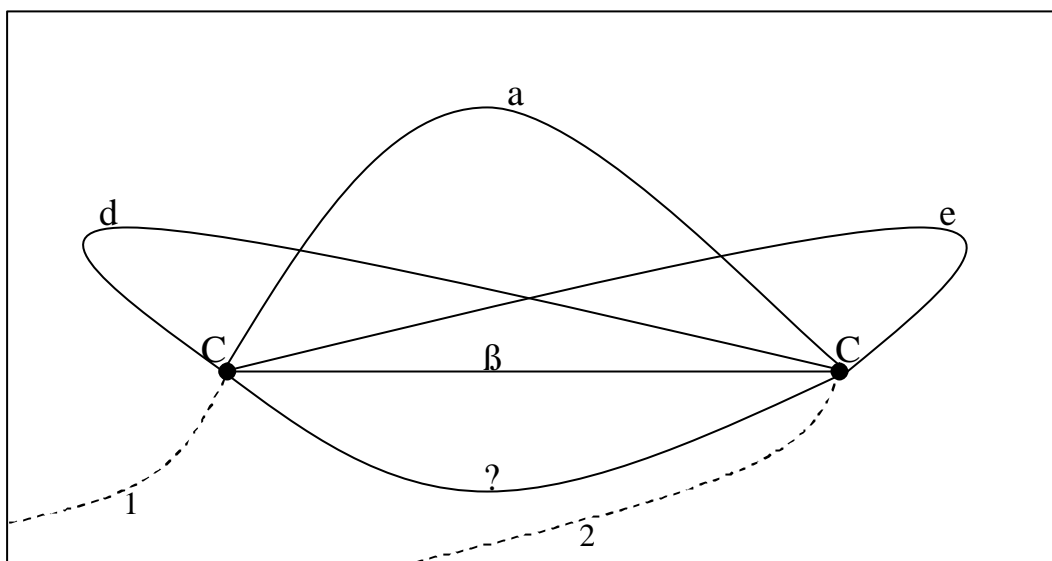


Figure 4.1 Five possible shapes critical curve (solid lines) of type I mixtures. Critical equilibria of binary mixtures (—), the critical points of the pure components (C), and the vapour pressure curves (1, 2 ---) are illustrated.

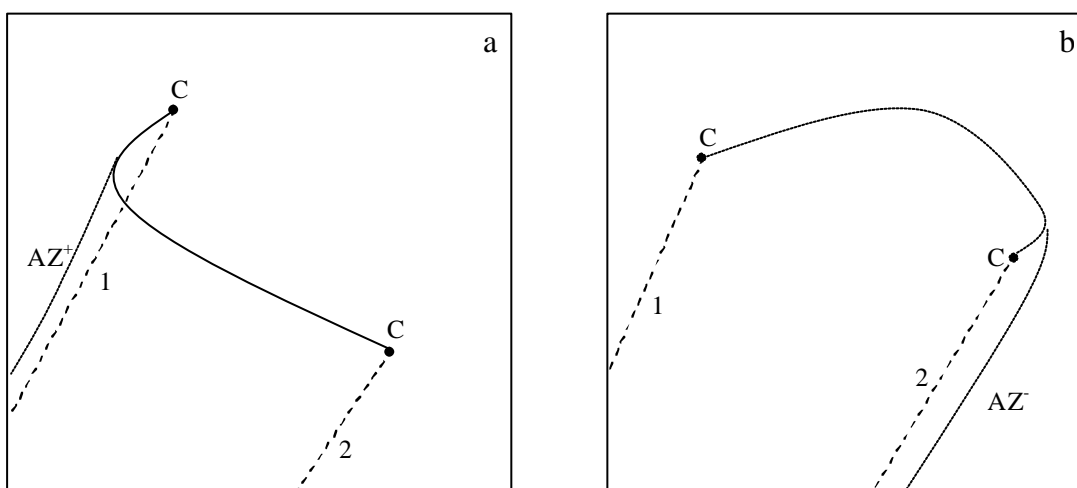


Fig 4.2 Two critical curves of type I which form a positive critical azeotrope (a) and a negative critical azeotrope (b). Both positive and negative azeotropic lines (...) are illustrated.

The critical curves of type I_d (curve d in Figure 4.1) which extends through a temperature minimum, is observed for several mixtures and is usually associated with the occurrence of a positive azeotrope extending up to the critical line in Figure (4.2a). The azeotropic line is given in the later. Typical examples are acetone + n

pentane, + n-hexane and + n-heptane, water + 1-propanol and carbon dioxide + ethane (Rowlinson and Swinton, 1982).

The critical curve of type I_e (curve e in Figure 4.1) extends through a temperature maximum before bending back to the critical point of the more volatile component and is also associated with the occurrence of a negative azeotrope extending up to the critical line in Fig. (4.2b). This means that there is partial phase immiscibility over a certain range of concentration, which immiscibility is occurring at temperatures higher than the critical temperature of both pure components. By common definition the substances in this region should thus be considered to be in the gaseous state and phase behaviour such as this is one example of so-called “gas-gas immiscibility”. The binary mixtures cycloheptane + tetraethylsilane (Hicks and Young, 1975) is an example of type I_e . Both type I_d and type I_e also are called type IA phase behaviour in which the azeotropic line is tangential to the projection of the critical locus but does not meet it at the temperature minimum in the global phase diagram.

4.1.2 Type II Phase Behaviour

Type II mixtures are characterized by the presence of liquid-liquid immiscibility at temperatures below the vapour-liquid critical temperature of the more volatile component. In addition, there is a continuous vapour-liquid curve which links the vapour-liquid critical points of component 1 and component 2. The extra liquid-liquid line extends down with either positive or negative slopes to low pressure, and terminates at an upper critical end point (UCEP). A three-phase line (LLV) extends from the UCEP to lower pressures and temperatures. There are three common

variations of type II phase behaviour as illustrated in Figure 4.3a. The distinction between these types depends on the shape of the LL lines (types II_a-II₇). Typical examples of type II are water + phenol (Roth, et al., 1966), CO₂ + n-C₈H₁₈ (van Konynenburg and Scott, 1980) and acetic acid + triethylamine (Rowlinson and Swinton, 1982).

There is only one possible azeotropic behaviour of type II, which is positive azeotropic behaviour, it is called type IIA in Figure 4.3b. Positive azeotropy is always limited azeotropy because the azeotropic line must disappear at low pressures at upper critical end point where it is tangent to a three-phase line LLV. An experimental example with positive azeotropy giving a type IIA phase diagram is the mixture CO₂ + C₂H₆.

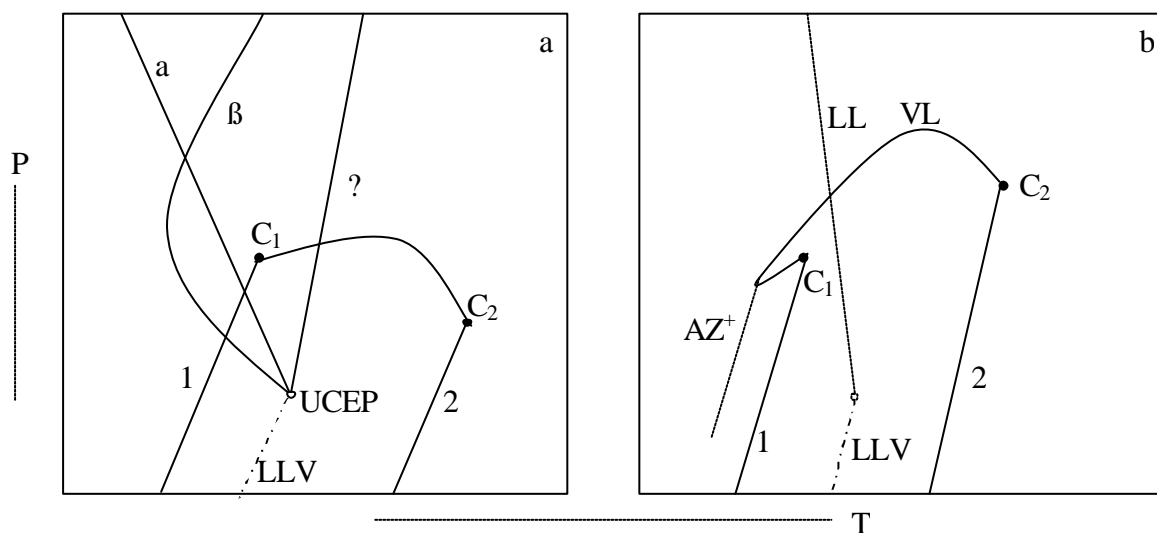


Figure 4.3. Type II and type IIA phase behaviour. UCEP is upper critical end point, three phase line liquid-liquid-vapour (— — —) is illustrated.

4.1.3 Type III Phase Behaviour

Type III mixtures have two distinct critical curves. One critical curve starts from the critical point of the pure component with the higher critical temperature and extends to high pressure. The other critical curve starts from the critical point of the other component with the lower critical temperature and extends to the UCEP on the end of a three-phase line. Five possible kinds of type III behaviour are depicted in Figure 4.4(a) p-T projections.

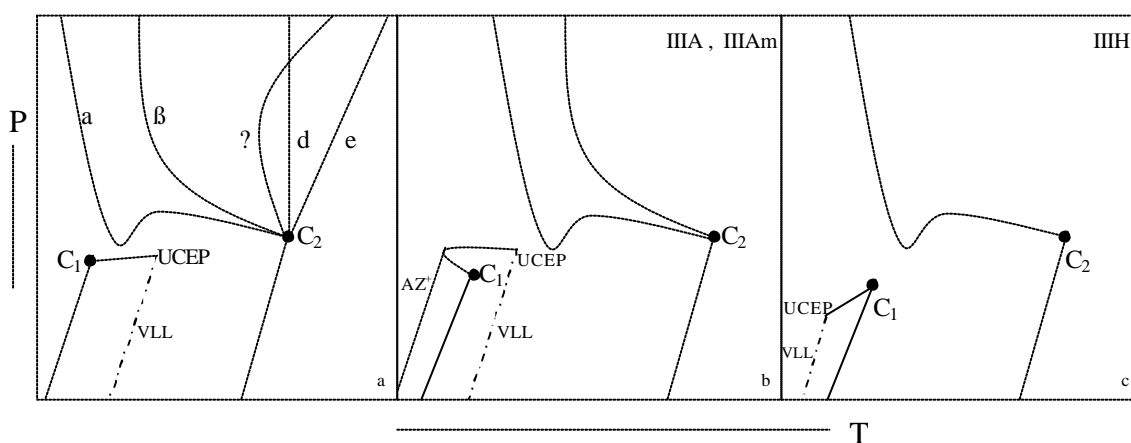


Figure 4.4 Type III, type IIIA and type IIIH phase behaviour.

In the global phase diagram, type III behaviour is also divided into five sub-types (Konynenburg and Scott, 1980, Deiters and Pegg, 1989, Yelash and Kraska, 1998). Type III_β-III_ε in Figure 4.4, are united to the general type III phase behaviour, and type III_α is incorporated into type III_m phase behaviour. The possibility of an azeotrope allows us to identify sub-classes of type III behaviour. Type III behaviour with the addition of an azeotrope is called type IIIA, and type IIIAm have both type IIIA and type III_m behaviour. These features of type III behaviour are illustrated in Figure 4.4b. In Figure 4.4(c), a three-phase line LLV runs from an UCEP to $p = 0$, T

= 0 at lower temperatures than the one pure component vapour-pressure curves, producing heteroazeotropic behaviour. The existence of a heteroazeotrope is signified by classifying this mixture as type IIIH.

In type III_a, the critical curve starts from the critical point of the component with the higher critical temperature, runs to direction of the critical point of the another component, passes through a pressure maximum and a pressure minimum, and then goes to very high pressure. Ethane + methanol (Brunner, 1985) is a typical type III_m mixture which has a pressure maximum and a pressure minimum in its critical curve that goes to infinite pressure.

The critical curve of a type III_β mixture has a negative slope whereas in type III_e mixture, it has a positive slope without a pressure maximum and minimum in the p-T projection. That is, the critical curve in type III_β extends to lower temperature whereas the critical curve in type III_e extends directly to higher temperature. In type III_γ behaviour, the critical curve only has a temperature minimum without a pressure minimum and a pressure maximum. Type III_d is also possible, the critical curve starts from the critical point of the component with the higher critical temperature and near vertically rises to very high pressure.

Binary systems of helium + xenon (de Swaan Arons and Diepen, 1966), water + neon (Mather et al., 1993) and water + helium (Sretenskaja et al., 1995) are type III_e mixtures, which show gas-gas equilibria without a minimum critical temperature. Water + argon (Tsiklis and Prokhorov, 1966; Lentz and Franck, 1969; Wu et al., 1990), water + xenon (Franck et al., 1974), water + krypton (Mather et al., 1993) and

ammonia + methane, argon or nitrogen (Brunner, 1988) are type III₂ mixtures. They display “gas-gas immiscibility” in which the critical line passes through a minimum in temperature. The helium + methane (Sinor et al., 1966; Streett, 1969) binary mixture is an example of type III_d critical phase behaviour.

4.1.4 Type IV Phase Behaviour

The p-T projection for type IV mixtures is illustrated in Figure 2.3 of Chapter 2 (Type IV). The critical line starting at the vapour-liquid critical point of the less volatile ends at a lower critical end point (LCEP) where it connects to the three-phase line. The critical locus thus changes its character continuously from vapour-liquid to liquid-liquid and provides a clear example of the confusion that can arise from a careless use of the words vapour and liquid in the critical region of a mixture. The three-phase line is quite short and ends at higher temperatures and pressures at a UCEP that connects, through a short critical line, with the vapour-liquid critical point of the more volatile pure component. A region of liquid-liquid immiscibility at temperatures below the vapour-liquid critical temperature of the more volatile component is also presented in type IV. The systems methane + 1-hexene (Davenport et al., 1966) and carbon dioxide + n-tridecane (van der Steen, 1989) are examples of systems showing type IV fluid phase behaviour.

4.1.5 Type V Phase Behaviour

Type V is similar to type IV but without the liquid-liquid critical line and the three phase line at lower temperature. An example of type V system is methane + n-hexane (Davenport and Rowlinson, 1963). In figure 4.5, the possible kinds of type V behaviour are shown. Type V with an azeotropic line is called type V_A phase behaviour (Figure 4.5 b). Recently, Boshkov and Yelash (1998), Yelash and Kraska (1998) and Wang et al. (2000), respectively, calculated another kind of type V mixture denoted as type V_m (Figure 4.5 c). A feature of type V_m behaviour is the presence of closed-loop liquid-liquid immiscibility.

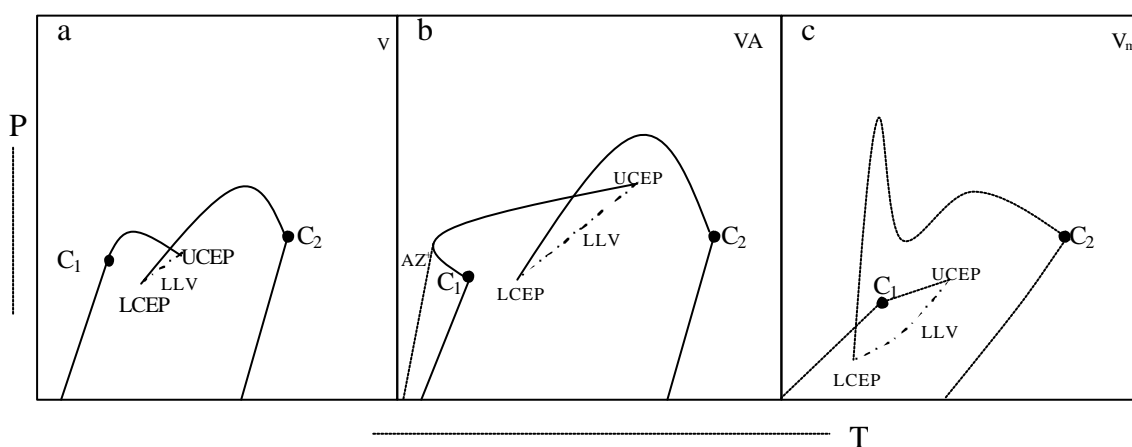


Figure 4.5 Type V, type V_A and type V_m phase behaviour.

4.1.6 Type VI and VII Phase Behaviour

Type VI phase behaviour consists of a liquid-vapour critical line connecting the two critical points of the pure components, and a liquid-liquid immiscibility critical line with a pressure maximum connecting both UCEP and LCEP of the same three-phase line. Another possibility is the existence of a second liquid-liquid critical curve at high

pressure with a pressure minimum. Type VII phase behaviour has the same liquid-liquid immiscibility critical line as type VI phase behaviour, but the liquid-vapour critical line is interrupted by a three-phase line. In Figure 4.6, type VI and type VII phase behaviour are illustrated.

Type VI phase behaviour can be found in the system water + 2-butoxyethanol (Schneider, 1963). Type VII phase behaviour has not been confirmed by experimental measurements. Boshkov (1987) reported type VII phase behaviour for Lennard-Jones mixtures of molecules of equal size. Yelash and Kraska (1998) and Wang et al. (2000) also obtained this phase behaviour for binary mixture of molecules of equal size using the Carnahan-Starling and Guggenheim equations of state, respectively.

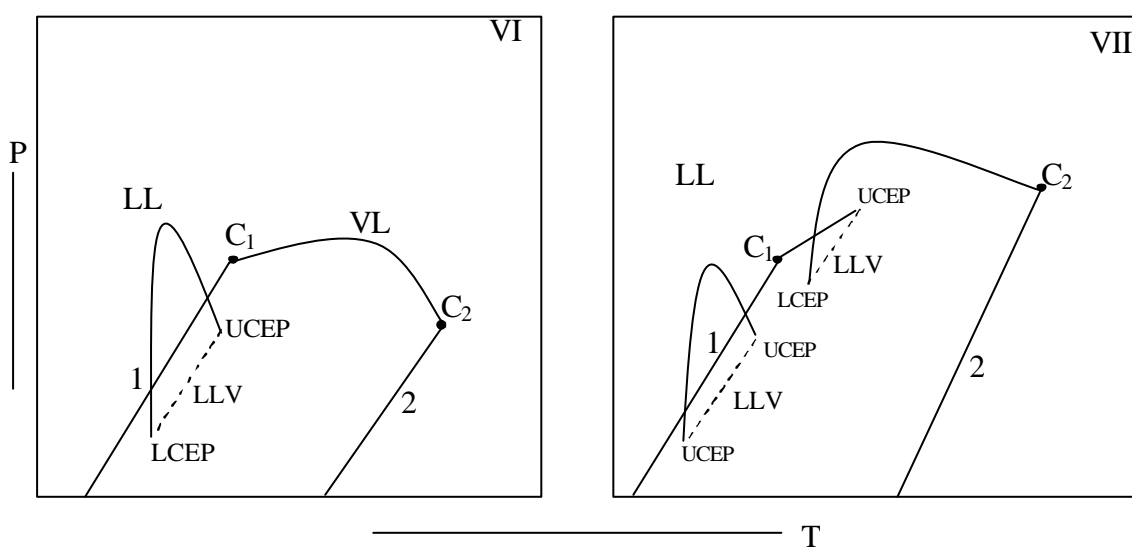


Figure 4.6. Type VI and type VII phase behaviour

4.1.7 Type VIII Phase behaviour

Type VIII mixtures (Fig. 4.7) have three distinct critical curves. One critical curve starts from the critical point of the pure component with the higher critical temperature and extends to high pressure. The other critical curve starts from the critical point of the other component with the low critical temperature and extends to the UCEP on the end of a three-phase line. The third critical curve is an extra liquid-liquid line extends down to low pressure from a very high pressure, and terminates at an LCEP.

The location of type VIII in the global phase diagram has not yet been exactly determined. Van Pelt et al. (1991) reported it in the binary system of $\text{CF}_4 + \text{NH}_3$.

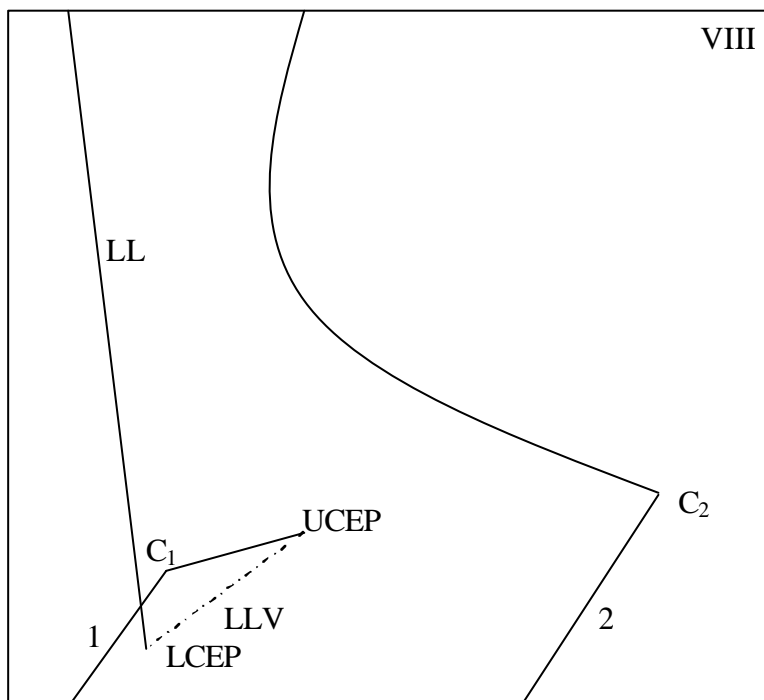


Figure 4.7 Type VIII phase behaviour

4.2 Boundaries Between Classes

The various phase diagram classes and the p-T projections of typical phase diagrams have been described in the previous section. In this section we describe the boundary states between phase diagram classes.

4.2.1 Azeotropic Critical End Points (ACEP)

A mixture of chemicals is azeotropic if the vapour composition is identical to that of the liquid phase. This means that the distillate of an azeotrope is theoretically identical to the solvents from which it is distilled.

The boundary lines between IIIA and IIIH is the azeotropic critical end point curves (ACEP). Deiters and Pegg (1989), Kraska and Deiters (1992) and van Pelt et al. (1995) calculated it by vdW, RK and SPHCT equations of state (see Chapter 3). ACEP is the curve when the critical endpoint and a critical azeotrope coincide (Kraska and Deiters, 1992). In IIIH behaviour, the UCEP is at a lower temperature than one of the pure component vapour-pressure curves. In type IIIA behaviour, the UCEP is at a higher temperature than one of the pure component vapour-pressure curves. Kraska and Deiters (1992) gave the condition of ACEP:

$$\frac{\partial p^c}{\partial V} = \frac{\partial p^c}{\partial x} = \frac{\partial^2 p^c}{\partial V^2} = 0, \quad \mathbf{m}_i^c = \mathbf{m}_i^a, \quad i = 1, 2. \quad (4.1)$$

where c denotes critical phase, a denotes the “auxiliary” equilibrium phase.

4.2.2 Tricritical Point (TCP) Line

The tricritical point (TCP) line is responsible for the distinction between the classes I and V, or II and IV, or VI and VII. The difference between these classes lies in the fact that in one case the critical point C_1 and C_2 is connected by a critical line, but in the other case the critical line is interrupted by a three-phase line. The transition state would be represented by a phase diagram where the three-phase line connecting the two critical lines in class V, IV, or VII shrinks to zero length at a tricritical point (TCP). Figure 4.8 shows that tricritical point as transition state between class I and V. Deiters and Pegg (1989) gave the mathematical criterion for a tricritical point, it is

$$G_{2x} = G_{3x} = G_{4x} = G_{5x} = 0 \quad (4.2)$$

where G is the molar Gibbs energy of a mixture, and G_{ixjT} is a shorthand notation for

$$G_{ixjT} = \left(\frac{\partial^{i+j} G}{\partial x^i \partial T^j} \right)_p \quad (4.3)$$

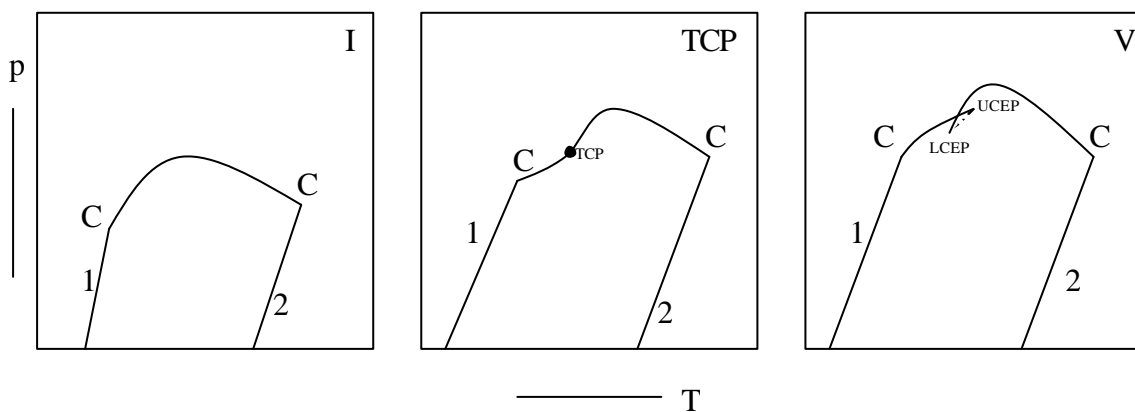


Figure. 4.8 Tricritical point as transition state between class I and V.

4.2.3 Double Critical End Points (DCEP)

When the critical lines of a class IV mixture are calculated, it often turns out that there are only two separate critical lines, rather than three. The critical line originating at high temperature critical point passes through a pressure minimum before going to high pressures. If the minimum lies below the three-phase line, or even at negative pressure, the critical line becomes unstable and appears to be interrupted, thereby producing class IV behaviour. This means that class IV is often a distorted class III_m. The transition state between class IV and class III_m, or VII and V_m or I and VI is a phase diagram where the critical line just touches the three-phase line, and forms a double critical end point (DCEP). Figure 4.9 illustrate the transition between type III and type IV behaviour via a DCEP.

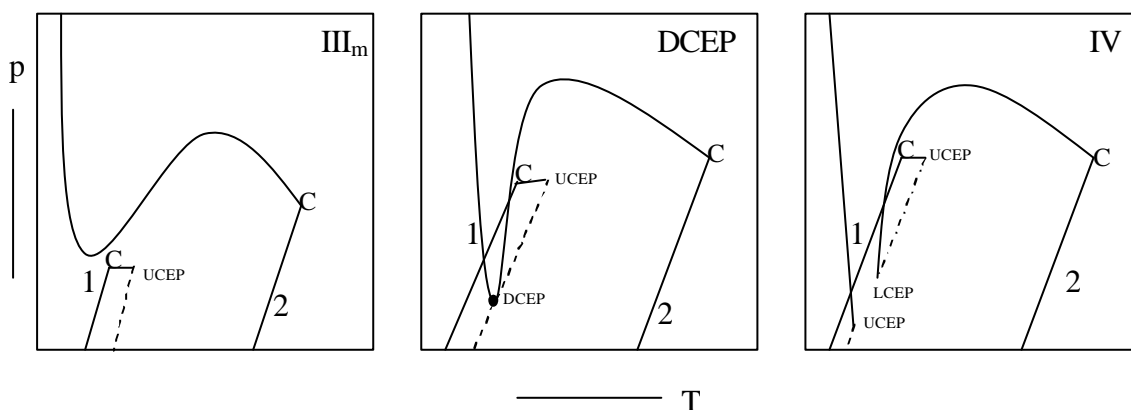


Figure. 4.9 Double critical end point as transition state between class III_m and IV.

At a double critical end point, there is a critical phase in equilibrium with another (noncritical) phase, and the slopes of the critical line and the three-phase line are the same. The mathematical criteria for a DCEP (Deiters and Pegg, 1989) are:

$$G_{2x}^c = G_{3x}^c = 0 \text{ (criticality)} \quad (4.4)$$

$$m_i^c = m_i^a \quad i = 1,2 \text{ (phase equilibrium)} \quad (4.5)$$

$$\frac{S_{2x}^c}{V_{2x}^c} = \frac{S_m^c - S_m^a - (x^c - x^a)S_x^c}{V_m^c - V_m^a - (x^c - x^a)V_x^c} \text{ (slope criterion)} \quad (4.6)$$

The notation for the derivatives S_x , S_{2x} , V_x and V_{2x} is analogous to that for G_{2x} . These derivatives must be calculated at constant pressure and temperature (Deiters and Pegg, 1989).

4.2.4 Critical Pressure Step Points (CPSP)

The critical pressure step point (CPSP) is a boundary state. At the CPSP, a critical pressure maximum and a critical pressure minimum coincide and vanish. This transition state occurs between class III and class III_m, or V and V_m. Figure 4.10 is an example of CPSP that is a transition state between class III and III_m.

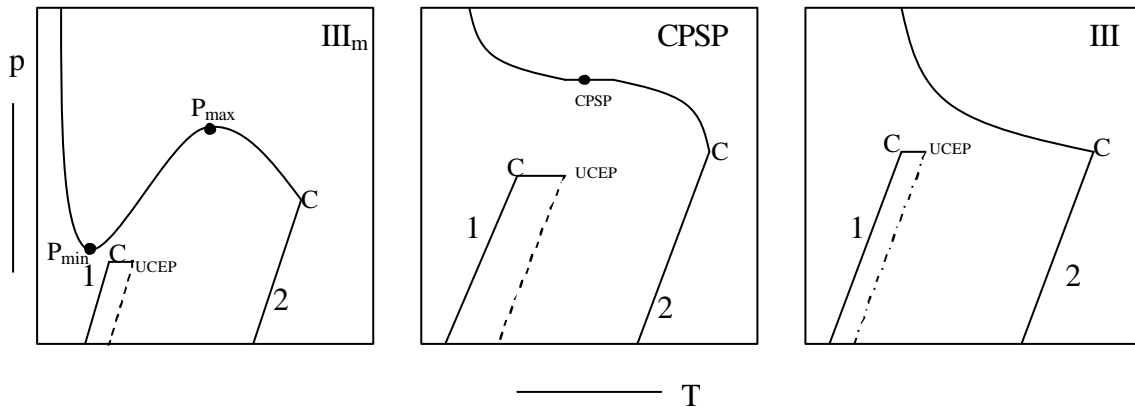


Figure. 4.10 critical pressure step point as transition state between class III_m and III.

The thermodynamic criterion of the CPSP has been derived by Boshkov and Yelash (1998) using a bifurcation method. The thermodynamic conditions are:

$$G_{2,x} = G_{3,x} = G_{2,x1T} = 0 \quad (4.7)$$

$$G_{4,x}G_{2,x2T} - (G_{3,x1T})^2 = 0 \quad (4.8)$$

4.2.5 Degenerated Critical Pressure Maximum or Minimum (dCPM)

The degenerated critical pressure maximum or minimum (dCPM) is another important boundary (Yelash and Kraska, 1998). The boundary is the pathway between V and III, or Vm and III_m, or VII and IV, or VI and II. A binary phase diagram with a dCPM is plotted in Figure 4.11. The dCPM line is called upper critical saddle point (UCSP) in the work of Kraska (1996).

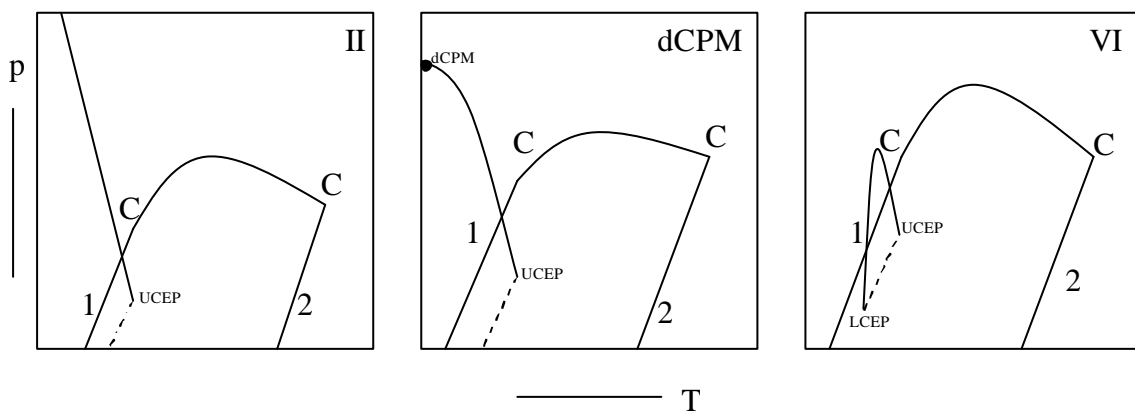


Figure. 4.11 dCPM as transition state between class II and VI.

The conditions for this state are Eq. (4.7) and $T = 0$. In practice a non zero but very small value for $T \rightarrow 0$ has been chosen (Yelash and Kraska, 1998).

4.2.6 The Van Laar Points

The DCEP curve and the TCP curve intersect at a point, which is called van Laar point (Meijer, 1989). For the vdW equation the van Laar point is located on the geometric mean curve (Meijer, 1989). The geometrical mean curve in the global phase diagram is defined as the semicircle curve which the center of the circle at point $(0.0, 1.0)$ of projection $\phi \sim \phi$, and the radius is 1.0. ϕ and ϕ are two parameters of topology (van Konynenburg and Scott, 1980), and will be given in the later. Meijer et al. (1989) have used this simplification to study the critical behaviour around the van Laar point analytically.

According to Kraska and Deiters (1992), the double critical end point curve of the Carnahan-Starling-Redlich-Kwong equation becomes metastable, before the van Laar point is reached. For the three-component lattice vapour (Furman et al., 1977; Furman and Griffiths, 1978), the double critical end point curve and the tricritical curve merge. Van Pelt and de Loos (1992) used the SPHCT equation to do extensive research on the structure of the critical curves in binary mixtures in the neighborhood of the van Laar point. In this region of the global phase diagram another important curve can be found (van Pelt et al., 1995) the mathematical double point (MDP) curve which lies between the curved TCP and DCEP curve in the global phase diagram. The MDP is a point in the V, T, x space of a binary mixture where the critical curve is self crossing (van Pelt et al., 1993). In the global phase diagram The MDP curve is not a

boundary between two types of phase behaviour. It goes through the van Laar point (van Pelt and de Loos, 1992) and is thermodynamically stable at the van Laar point only.

4.2.7 Double Critical End Cusp (DCEC)

The double critical end cusp (DCEC) is a cusp of the DCEP lines in the global phase diagram. The possible binary phase diagram of DCEC in Figure 4.12 is that a critical line goes tangentially to a three-phase line at the critical end point. In the loci of DCEC, there are type V, V_m and VII in the global phase diagram. Yelash and Kraska (1998) gave the thermodynamic criterion of the DCEC:

$$\frac{D(\Lambda_G, \Delta G_x, G_{2x}, G_{3x}, \mathfrak{R}^{DCEP})}{D(x^a, x^c, T, p, \Gamma)} = 0 \quad (4.9)$$

Eq. (4.9) is the general Jacobian express function. The functions of Λ_G , ΔG_x and \mathfrak{R}^{DCEP} in Eq. (4.9) are:

$$\Lambda_G \equiv G^a - G^c - (x^a - x^c)G_x^c \quad (4.10)$$

$$\Delta G_x \equiv G_x^a - G_x^c \quad (4.11)$$

$$\mathfrak{R}^{DCEP} = \frac{G_{2x1T}^c}{G_{2x1p}^c} - \frac{G_T^c - G_T^a - (x^c - x^a)G_{1x1T}^c}{G_p^c - G_p^a - (x^c - x^a)G_{1x1p}^c} \quad (4.12)$$

The symbol of ? stands for one of ?, ?, ? and ? which are four parameters of topology (van Konynenburg and Scott, 1980) in vdW global phase diagram.

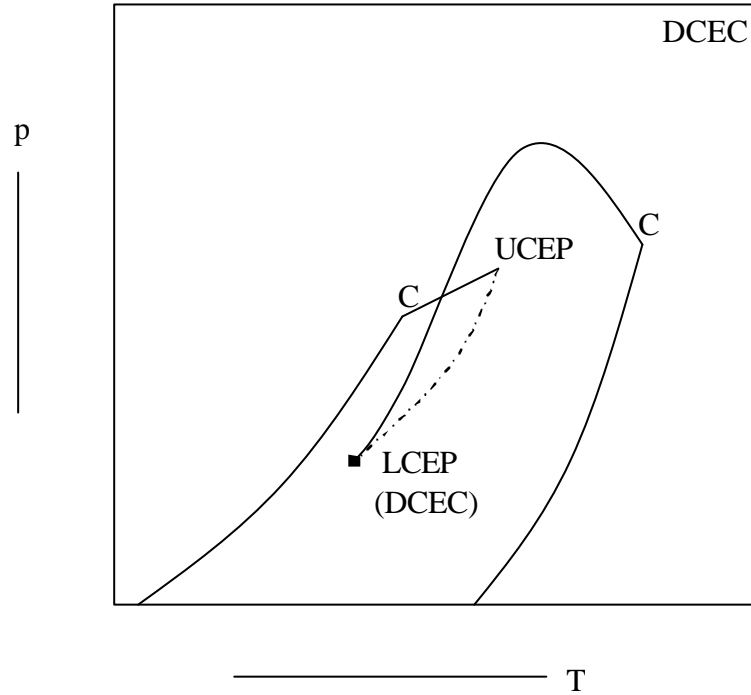


Figure 4.12 The possible binary phase diagram of double critical end cusp (DCEC)

4.2.8 Critical Pressure Landing Point (CPLP)

The CPLP is a cusp of the CPSP lines in the global phase diagram. In Figure 4.13, an example of a CPLP is shown. The top of critical line, which starts from the higher temperature critical point is very flat. In the global phase diagram, the locus of CPLP has type V and V_m .

Boshkov and Yelash (1998) gave the thermodynamic description of the CPLP,

$$\mathfrak{R}^{CPLP} \equiv \mathfrak{R}_x^{CPSP} G_{2 \times 2T} - \mathfrak{R}_T^{CPSP} G_{3 \times 1T} = 0 \quad (4.13)$$

where \mathfrak{R}_x^{CPSP} and \mathfrak{R}_T^{CPSP} are the derivatives of the CPSP criterion Eq. (4.8) with respect to composition and temperature:

$$\mathfrak{R}_x^{CPSP} = G_{5x} G_{2x2T} + G_{3x2T} G_{4x} - 2G_{4x1T} G_{3x1T} \quad (4.14)$$

$$\mathfrak{R}_T^{CPSP} = G_{4x1T} G_{2x2T} + G_{2x3T} G_{4x} - 2G_{3x2T} G_{3x1T} \quad (4.15)$$

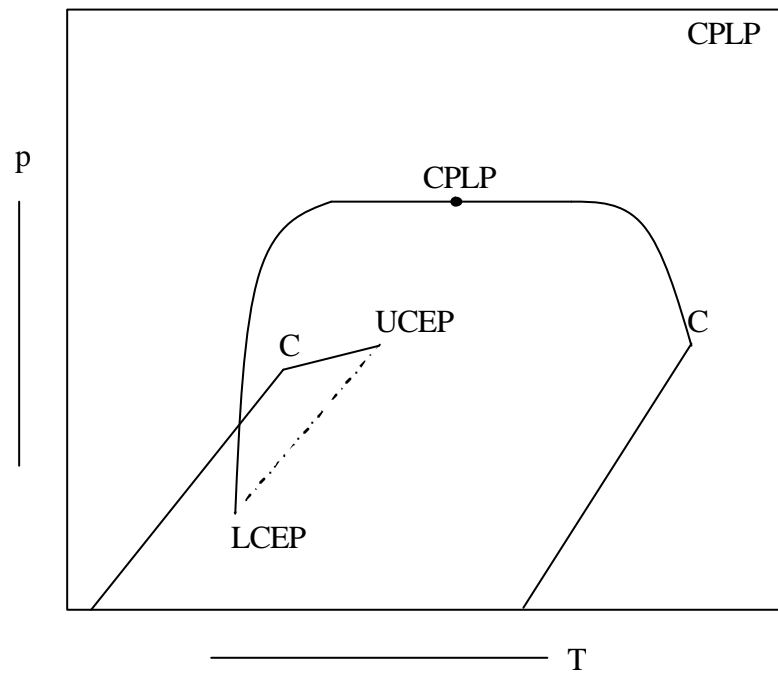


Figure 4.13 The binary diagram of critical pressure landing point (CPLP).

4.3 Global Phase Diagram

Global phase diagrams are calculated using equations of state with suitable mixing rules. The first global phase diagram was proposed by Konynenburg and Scott (1980) using the vdW equation of state for the systematic investigation of all possible kinds of phase diagrams in binary mixtures. It was convenient to describe the mixtures with three new topology parameters, z , l , and h (van Konynenburg and Scott, 1980). Other authors (Deiters and Pegg, 1989; Kraska and Deiters, 1992) defined additional topology parameter called x , and replaced parameter z with symbol z . These parameters are dimensionless, and they are defined as:

$$z = \frac{d_{22} - d_{11}}{d_{22} + d_{11}} \quad (4.16)$$

$$l = \Lambda = \frac{d_{22} - 2d_{12} + d_{11}}{d_{22} + d_{11}} \quad (4.17)$$

$$x = \frac{b_{22} - b_{11}}{b_{22} + b_{11}} \quad (4.18)$$

$$h = \frac{b_{22} - 2b_{12} + b_{11}}{b_{22} + b_{11}} \quad (4.19)$$

Where d_{ij} in Eq. (4.16) and Eq. (4.17) is the interaction density which is related to the equation of state attraction parameter a_{ij} . Deiters and Pegg (1989) gave the definition of d_{ij} ,

$$d_{ij} = \frac{T_{ij}^* b_{ij}}{b_i b_{ij}} \quad (4.20)$$

$$T_{ij}^* = \frac{a_{ij}}{8Rb_{ij}} \quad (4.21)$$

where b_{ij} is the equation of state covolume parameter which is related to the size of the molecules.

The global phase diagram is divided into several different regions by boundary lines such TCP, DCEP, AZ, dCPM, ACEP and CPSP, etc, in topology parameters τ - τ projection. A τ - τ global phase diagram is given in Figure 4.14 for binary mixtures of equal sized molecules.

In the Fig. 4.14, the small triangle in the top of the diagram is called the 'shield region' (Furman and Griffiths, 1978). It was first discovered for a symmetrical three-component system by Furman et al. (1977), and later modified by Furman and Griffiths (1978) for a van der Waals binary mixture. Type IIA, III_m and III_H are found in this area. Type IIA has more than one liquid-liquid critical line, and the type III behaviour also has a extra liquid-liquid critical curve found (van Konynenburg and Scott, 1980).

The big triangle shield-region in the middle of upper half of the diagram in Figure 4.11 is closed by double critical end points (DCEP) curves. It was first discovered by van Konynenburg and Scott (1980) who found type II, IIA and IV in this area with

van der Waals equation of state. Yelash and Kraska (1998) examined the area with Carnahan-Starling-van der Waals equation of state, and found closed-loop phase behaviour of type VI and VII in this region.

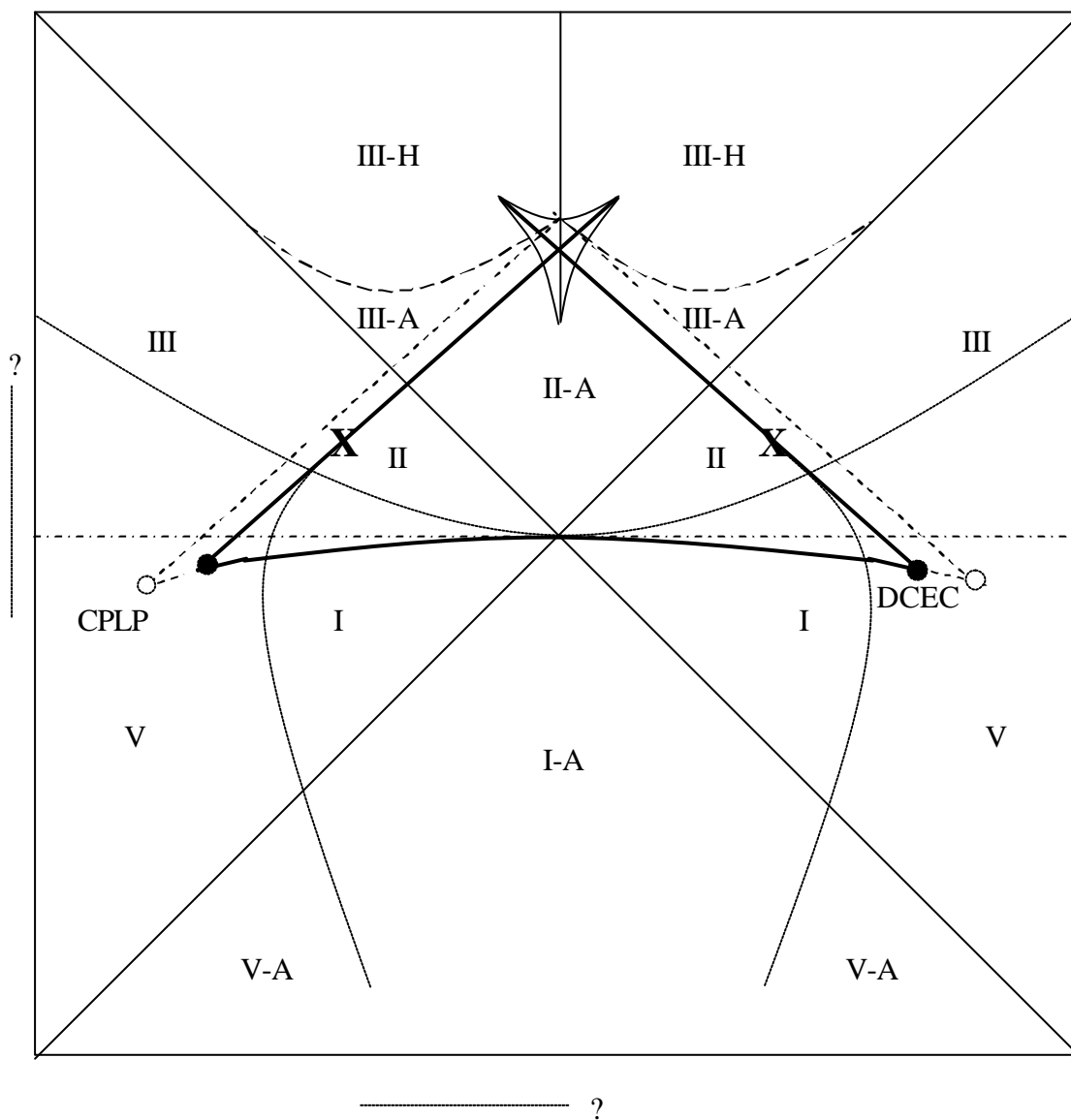


Figure 4.14 The global phase diagram (Yelash and Kraska, 1998) of the binary CSvdW-fluid for equal sized molecules. Double critical end point (?) curves, Azeotropic critical end points (---) curves, Tricritical point (—) curves and critical pressure step point (---) curves are illustrated.

The diagonal lines (Figure 4.14) are boundary states of the critical azeotropy (AZ) which separate type II and IIA, or type I and IA. The areas of the type IIIA and IIIH

are separated by lines of azeotropic critical end points (ACEP). The dashed curves are lines of the critical pressure step point (CPSP), which is the boundary line between type III and III_m, or V and V_m. The crosses mark the van Laar points. The solid curves going from the van Laar points into the lower half of diagram are parts of lines of the tricritical points (TCP). The symmetric TCP line is marked with the vertical solid line going from the lower corner of the big shield region to the top of the diagram, and separate type II and IV, or type VI and VII, or type I and V.

For the global phase diagram of equal sized molecules ($\chi = 0$), the diagram in the ϕ - ϕ projection is same both part of positive ϕ and part of negative ϕ . However, significant changes occur for mixtures of molecules of different size. These changes are particularly apparent in the corner of the big triangle shield-region in Figure 4.14.

If the parameter $\phi > 0$ ($\chi \in (-1, 1)$), the big triangular shield-region in Figure 4.14 moves to left, and the left corner of the kite-shaped figure is changed (van Konynenburg and Scott, 1980; Deiters and Pegg, 1989; Kraska and Deiters, 1992; van Pelt et al., 1995). The bigger of the value of $|\phi|$, the more the triangle region will move to left or right, and the left or the right corner of the triangle will be changed more.

References

- Boshkov, L. Z. and Yelash, L. V. (1998). Closed-loops of Liquid-Liquid Immiscibility in Binary Mixtures Predicted from the Redlich-Kwong Equation of State, *Fluid Phase Equilib.*, **141**, 105-112.
- Brunner, E. (1985). Fluid Mixtures at High Pressures II. Phase Separations and Critical Phenomena of (ethane + an n-alkanol) and of (ethane + methanol) and of (propane + methanol), *J. Chem. Thermodyn.*, **17**, 871-885.
- Brunner, E. (1988). Fluid Mixtures at High Pressures VII. Phase Separations and Critical Phenomena in 12 Binary Mixtures Containing Ammonia, *J. Chem. Thermodyn.*, **20**, 1379-1409.
- Davenport, A. J. and Rowlinson, J. S. (1963). The Solubility of Hydrocarbons in Liquid Methane, *Trans. Faraday Soc.*, **59**, 78-84.
- Davenport, A. J., Rowlinson, J. S. and Saville, G. (1966). Solution of Three Hydrocarbons in Liquid Methane, *Trans. Faraday Soc.*, **62**, 322-327.
- De Swaan Arons, J. and Diepen, G. A. M. (1966). Gas-Gas Equilibria, *J. Chem. Phys.*, **44**, 2322-2300.
- Deiters, U. K. and Pegg, I. L. (1989). Systematic Investigation of the Phase Behaviour in Binary Fluid Mixtures. I. Calculations Based on the Redlich-Kwong Equation of State, *J. Chem. Phys.* **90**, 6632-6641.
- Franck, E. U., Lentz, H. and Welsch, H. (1974). The System Water-Xenon at High Pressures and Temperatures, *Z. Phys. Chem. (Frankfurt am Main)*, **93**, 95-108.
- Furman, D. Dattagupta, S. and Griffiths, P. B. (1977). Global Phase Diagram for Three-Component Model, *Phys. Rev. B*, **15**, 441-464.
- Furmann, D. and Griffiths, R. B. (1978). Global Phase Diagram for a Van der Waals Model of a Binary Mixture, *Phys. Rev. A*, **17**, 1139-1148.

- Hicks, C. P. and Young C L. (1975). The Gas-Liquid Critical Properties of Binary Mixtures, *Chem. Rev.*, **75**, 119-175.
- Imre, A. R., Melnichenko, G. and Alexander van Hook, W. (1999). Liquid-Liquid equilibria in Polystyrene Solutions: the General Pressure Dependence, *Phys. Chem. Chem. Phys.*, **1**, 4287-4292.
- Kolafa, J., Nezbeda, I., Pavlíček, J. and Smith, W. R. (1998). Global Phase Diagrams of Model and Real Binary Fluid Mixtures: Lorentz-Berthelot Mixture of Attractive Hard Spheres, *Fluid Phase Equilib.*, **146**, 103-121.
- Kolafa, J., Nezbeda, I., Pavlíček, J. and Smith, W. R. (1999). Global Phase Diagrams of Model and Real Binary Fluid Mixtures Part II. Non-Lorentz-Berthelot Mixtures of Attractive Hard Spheres, *Phys. Chem. Chem. Phys.*, **1**, 4233-4240.
- Kraska, T. and Deiters, U. K. (1992). Systematic Investigation of the Phase Behaviour in Binary Fluid Mixtures. II. Calculations Based on the Carnahan-Starling-Redlich-Kwong Equation of State, *J. Chem. Phys.*, **96**, 539-547.
- Kraska, T. (1996). Systematic Investigation of the Global Phase Behaviour of Associating Binary Fluid Mixtures : I. Mixtures Containing One Self-Associating Substance, *Ber. Bunsenges. Phys. Chem.*, **100**, 1318-1327.
- Lamm, M. H. and Hall, C. K. (2001). Molecular Simulation of Complete Phase Diagrams for Binary Mixtures, *AIChE J.*, **47**, 1664-1675.
- Lentz, H. and Franck, E. U. (1969). Water-Argon System at High Pressures and Temperatures, *Ber. Bunsenges. Phys. Chem.*, **73**, 28-35.
- Mather, A. E., Sadus, R. J. and Franck, E. U. (1993). Phase Equilibria in (Water + Krypton) at Pressures from 31 MPa to 273 MPa and Temperatures from 610K to 660K and in (Water + Neon) from 45MPa to 255MPa and from 660K to 700K, *J. Chem. Thermodyn.*, **25**, 771-779.

- Meijer, P. H. E. (1989). The van der Waals Equation of State around Van Laar Point, *J. Chem. Phys.*, **90**, 448-456.
- Muirbrook, N. K. and Prausnitz, J. M. (1965). Multicomponent Vapour-Liquid Equilibria at High Pressures. I. Experimental Study of the Nitrogen-Oxygen-Carbon Dioxide System at 0°C, *AIChE. J.*, **11**, 1092-1096.
- Polishuk, I., Wisniak, J., Segura, H., Yelash, L. V. and Kraska, T. (2000). Prediction of the Critical Locus in Binary Mixtures Using Equation of State. II. Investigation of van der Waals-Type and Carnahan-Starling-Type Equation of State, *Fluid Phase Equilib.*, **172**, 1-26.
- Polishuk, I., Wisniak, J. and Segura, H. (2002). Closed Loops of Liquid-Liquid Immiscibility Predicted by Semi-Empirical Cubic Equations of State and Classical Mixing Rules, *Phys. Chem. Chem. Phys.*, **4**, 879-883.
- Prausnitz, J. M., Lichtenthaler, R. N. and de Azevedo, E. G. (1999). Molecular Thermodynamics of Fluid-Phase Equilibria, 3^d Ed., Prentice Hall, Upper Saddle River, N. J..
- Roth, K., Schneider G. M. and Franck, E. U. (1966). Liquid-Liquid and Liquid-Solid Phase Equilibria in Cyclohexane-Methanol and Phenol-Water Systems up to 6000 bars, *Ber. Bunsenges. Phys. Chem*, **70**, 5-10.
- Rowlinson, J. S. and Swinton, F. L. (1982). Liquids and Liquid Mixtures, 3^d Ed., Butterworths, London.
- Sadus, R. J. (1992). High Pressure Phase Behaviour of Multicomponent Fluid Mixtures, Elsevier, Amsterdam.
- Schneider, G. M. (1963). Pressure Influence on the Separation of Liquid Systems. I. Closed Miscibility Gaps up to 5000 bars, *Z. Phys. Chem. NF.*, **37**, 333-352.

- Schouten, J. A., Deerenberg, A. and Trappeniers, N. J. (1975). Vapour-Liquid and Gas-Gas Equilibria in Simple Systems. IV. System Argon-Krypton, *Physica*, **81A**, 151-160.
- Sinor, J. E., Schindler, D. L. and Kurata, F. (1966). Vapour-Liquid Phase Behaviour of the Helium-Methane System, *AIChE. J.*, **12**, 353-357.
- Sretenskaja, N. G., Sadus, R. J. and Franck, E. U. (1995). High Pressure Phase Equilibria and Critical Curve of the Water + Helium System to 200 MPa and 723K, *J. Phys. Chem.*, **99**, 4273-4277.
- Streett, W. B. (1969). Gas-Liquid and Fluid-Fluid Phase Separation in the System Helium + Argon at High Pressure, *Trans. Faraday Soc.*, **65**, 696-702.
- Stryjek, R., Chappellear, P. S. and Kobayashi, R. (1974). Low-Temperature Vapour-Liquid Equilibria of Nitrogen-Methane System, *J. Chem. Eng. Data*, **19**, 334-339.
- Tsiklis, D. S. and Prokhorov, V. M. (1966). Mutual Limited Solubility of Gases in the System Water-Argon, *Zh. Fiz. Khim. USSR*, **40**, 2335-2337.
- Wichterle, I. and Kobayashi, R. (1972). Vapour-Liquid Equilibrium of Methane-Ethane System at Low Temperatures and High Pressures, *J. Chem. Eng. Data*, **17**, 9-12.
- Wu, G., Heilig, M., Lentz, H. and Franck, E. U. (1990). High Pressure Phase Equilibria of the Water-Argon System, *Ber. Bunsenges. Phys. Chem.*, **94**, 24-27.
- Van der Steen, J., de Loos, Th. W. and de Swaan Arons, J. (1989). The Volumetric analysis and Prediction of Liquid-Liquid-Vapour Equilibria in Certain Carbon Dioxide + n-Alkane Systems, *Fluid Phase Equilib.*, **51**, 353-367.
- Van Pelt, A. and de Loos, Th. W. (1992). Connectivity of Critical Lines Around the van Laar Point in T, X Projections, *J. Chem. Phys.*, **97**, 1271-1281.

- Van Pelt, A., Peters, C. J. and de Swaan Arons, J. (1991). Liquid-liquid Immiscibility Loops Predicted with the Simplified-perturbed-hard-chain Theory, *J. Chem. Phys.*, **95**, 7569-7576.
- Van Pelt, A., Peters, C. J., de Swaan Arons, J. and Meijer, P. H. E. (1993). Mathematical Double Points According to the Simplified-Perturbed-Hard-Chain Theory, *J. Chem. Phys.*, **99**, 9920-9929.
- Van Pelt, A., Peters, C. J. and de Swaan Arons, J. (1995). Global Phase Behavior Based on the Simplified-Perturbed Hard-Chain Equation of State, *J. Chem. Phys.*, **102**, 3361-3375.
- Van Konynenburg, P. H. and Scott, R. L. (1980). Critical Lines and Phase Equilibria in Binary van der Waals Mixtures, *Philos. Trans. Roy. Soc. London A*, **298**, 495-540.
- Wang, J. L., Wu, G. W. and Sadus, R. J. (2000). Closed-Loop Liquid-Liquid Equilibria and the Global Phase Behaviour of Binary Mixtures Involving Hard-Sphere + van der Waals Interactions, *Mol. Phys.*, **98**, 715-723.
- Yelash, L. V. and Kraska, T. (1998). Closed-Loops of Liquid-Liquid Immiscibility in Binary Mixtures of Equal Sized Molecules Predicted with a Simple Theoretical Equation of State, *Ber. Bunsenges. Phys. Chem.*, **102**, 213-223.
- Yelash, L. V. and Kraska, T. (1999). The Global Phase Behaviour of Binary Mixtures of Chain Molecules: Theory and Application, *Phys. Chem. Chem. Phys.*, **1**, 4315-4322.
- Young, C. L. (1986). Phase Equilibria in Fluid Mixtures at High Pressures, *Pure & Appl. Chem.*, **58**, 1561-1572.